Nanotechnology Perceptions
ISSN 1660-6795
www.nano-ntp.com

Analysis of Non-Uniform Transmission Lines with Different Distributed Parameters

Krishna Kumar Srivastav[1], Hitendra Singh[2], Vikas Kumar Shukla[3]

[1]*Research Scholar, Maharishi School of Science & Humanities, MUIT, Lucknow*
[2]*Assistant Professor, Maharishi School of Engineering and Technology, MUIT, Lucknow*
[3]*Assistant Professor, Maharishi School of Science & Humanities, MUIT, Lucknow*

The perturbation method proves successful in approximating the analysis of non-uniform transmission lines, given that the amplitudes of the distributed parameters remain within a reasonable range. Furthermore, the research explores the most far-reaching generalization of this work, which involves considering non-linear dependencies of the distributed parameters on voltage and current histories, as well as non-uniform transmission lines with randomly fluctuating parameters. The modeling file associated with this research validates the parameters discussed in the analysis. The simulation results indicate a linear output frequency response from the beginning, signifying a stable output with minimal distortion. The perturbation technique offers a powerful tool to approximate the solutions of the coupled differential equations, enabling engineers to understand and design transmission lines more effectively. The findings presented in this thesis can be applied to various areas such as power systems, telecommunications, and signal transmission, where non-uniform transmission lines play a crucial role.

Keywords: B Non-uniform transmission line, subharmonic currents, Series Capacitance, voltage protection etc.

1. Introduction

Finding answers to the challenges facing power systems is the purpose of this study, which was introduced previously and explained in more detail. These compensators are capable of being connected to the rest of the system in one of two distinct ways: either in series or in shunt at the terminals of the line (or even in the midpoint). There are three different types of constraints that may be placed on the loading capacity of a transmission system: (1) Thermal, (2) Dielectric and (3) Stability

Compensation of the Load in the Power System is the most effective method for increasing the system's capacity to transmit power and enhancing the voltage stability of the system. Operating the system such that the power factor is as close to one as possible is desirable from both an economic and a technical standpoint This will cut down on the flow of negative sequence currents, which will ultimately lead to an increase in the system's load capacity and a decrease in power loss. There are three types of critical loadings for a transmission line.

- Natural loading
- The limit on the steady-state stability and
- Loads at the thermal limit.

The natural loading on a compensated line is the lowest, and the steady-state stability limit is obtained at before the thermal loading limit is reached.

If the voltage profile is not flat, then the transmission line is not functioning properly. Even if this may not be achievable, it is still possible to attain the optimum voltage profile by modifying the characteristics of the line using line compensators. This will allow for the optimal voltage profile to be achieved.

- The Ferranti effect is reduced to a minimum
- It is not necessary to run synchronous generators with the under excited operating mode.
- The capacity of the line to transmit electricity is improved after the upgrade. Line compensation refers to the process of modifying the properties of a line or lines.

The following are some of the compensatory devices:

- Capacitors
- Electromechanical capacitors and inductors
- A source of voltage that is active (synchronous generator)

Switching allows for incremental adjustments to be made to a bank of capacitors and/or inductors (mechanical). The terms "passive line compensators" refer to capacitors and inductors in and of themselves, whereas "active line compensators" refer to synchronous generators. Before moving on to the more in-depth explanation of the line compensator, we are going to have a quick conversation on both shunt and series compensation.

Shunt compensation may be thought of as being analogous to load compensation, complete with all of the benefits that come along with it. It is imperative that this point be emphasised because shunt capacitors and inductors cannot be placed in a consistent fashion throughout the line. Typically, they are linked at the terminal end of the line or at the point exactly in the middle of the line.

Because shunt capacitors enhance the load pf, the line does not need to carry the reactive power, which results in a significant increase in the amount of power that can be transferred across the line. It is possible to increase the power that is transferred by shunt compensation, but only up to a certain point since doing so would need a capacitor bank of a very high size,

which would be impractical. There are additional and superior methods that may be used to increase the amount of electricity that is transferred down the line. As an illustration, series compensation, increased transmission voltage, HVDC, and so on are all examples.

When switched capacitors are used for compensation, it is important to disconnect them as soon as possible whenever there is a light load. This will help prevent an excessive increase in voltage as well as ferro resonance when transformers are present.

Through the use of series capacitors, the series inductive reactance of the line is partially nullified so that series compensation may fulfil its function. This assists in I increasing the maximum amount of power that can be transferred, (ii) decreasing the power angle for a certain amount of power that can be transferred, and (iii) loading more. It is preferable, from a purely practical standpoint, to keep the total amount of series compensation below or at 80 percent. Economic considerations and the intensity of the fault currents play a role in determining the placement of series capacitors. A capacitor connected in series lowers the line reactance and, as a result, the amount of fault currents.

2. COMPENSATION IN SERIES USED IN POWER SYSTEMS

Compensation Paid in Series - Controlling the effective reactance between line ends may be accomplished by connecting a capacitor in series with the line. This effective reactance may be calculated using

$$X_l' = X - X_c$$

were

- X_l = line reactance
- X_C = capacitor reactance

A reduction in the effective line reactance may be shown to be caused by the capacitor quite easily. This causes an improvement in the system's performance, as can be seen in the table below.

1. The voltage drop in the line is reduced (gets compensated), which results in a reduction in the amount of fluctuation in the end voltage.
2. Prevents voltage breakdown.
3. The steady-state power transfer goes up; it has an inverse relationship to X'l.
4. As a consequence of the preceding point, the transient stability limit rises.

The series capacitor compensator has a number of advantages, but it also has a number of drawbacks. The capacitive reactance is described here. When combined with the total series reactance, XC creates a series resonant circuit.

$$X = X_l + X_{\text{gen}} + X_{\text{trans}}$$

The natural frequency of oscillation of this circuit is given by

$$f_C = \frac{1}{2\pi\sqrt{LC}}$$

$$= \frac{1}{2\pi\sqrt{\frac{X}{2\pi f}\frac{2\pi f C}{2\pi f}}} = f\sqrt{\frac{X_C}{X}}$$

Where

f = system frequency

$\frac{X_C}{X}$ = degree of compensation

= 25 to 75% (recommended)

For this degree of compensation

$$f_C < f$$

3. OVER VOLTAGE PROTECTION OF SERIES CAPACITOR

This is because it is only then that it is necessary to accommodate the series compensation. On the other hand, the overvoltage protection of the series capacitor may be able to remove the capacitor from the faulty circuit. A Spark Gap (SG), a Metal Oxide Varistor (MOV), or both, together with a bypass circuit breaker, is the standard method for protecting a capacitor from an excessive amount of voltage. This method is shown in Figure 3. Because of this, there are two distinct impedance states that occur during a fault:

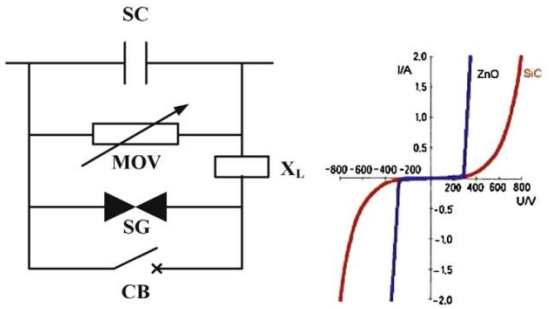

Figure 1: Over voltage protection of series compensator and MOV characteristic

If there is a fault situation that involves a high current, the voltage across the capacitor will rise to an extremely high value, which will cause the MOV to conduct and bypass the capacitor. In this scenario, the impedance of the SC–MOV combination will be lowered to the impedance of the MOV by itself. Even though there was only a little amount of current flowing through the fault, The impedance provided by the SC–MOV combination is equivalent to that provided by the parallel combination of the pair.

There are two different impedance circumstances that make relay configuration more challenging. Without taking into account the MOV conduction, the placement of a relay runs

the risk of overreaching and quickly losing its directional integrity. It is possible for the relay to underreach under low fault situations if the parameters are changed while continuing to take MOV into persistent account.

4. LITERATURE REVIEW

Jagadeesh Kumar, egtal. (2022), Linearly, the demand for electricity and the amount of money lost in the transmission sector are growing. Transmission lines are experiencing voltage fluctuation owing to an increase in the utilisation of nonlinear loads. The sag, swell, voltage spikes, harmonics, open and short circuit faults are some of the issues. Swell and sag are two of the most serious problems with power quality, and the interline dynamic voltage restorer may help fix them (IDVR). As long as IDVR is able to execute voltage compensation at a sufficient pace, it provides a constant energy supply across the DC link capacitance. Several DVRs linked to different distribution feeders in the electrical system may share a common energy storage, according to this strategy. When DVR needs correction, a SMES is used to provide power to the superconducting magnetic energy storage system (SMES). Additionally, fuzzy logic control was included. The suggested method's efficiency and performance are shown in the Simulink results.

Saad, M., & Kim, C. H. (2022), For shunt-compensated extra-high-voltage transmission lines, this research presents a unique adaptive reclosing method with two stages. First, a criteria for measuring the exact moment of secondary arc extinction is devised, called the SAEPC (Secondary Arc Extinction Peak-Based Criteria). The method is based on the estimated weighted lower-order harmonics and the size of the defective phase voltage. In the second step of fault classification, the harmonics root mean square factor (HRF) is reported, i.e. temporary or permanent. The suggested method not only detects the quenching moment but also recognises the kind of fault, independent of fault location, compensation level, or arc extinction speed. It has been shown that the suggested method is able to overcome the restrictions of current single-criterion harmonics-based reclosing methods.

Paul, S., etal. (2021), Vibration de-icing robots in power transmission lines may be powered up using an electromagnetic energy harvester (EMEH) that was developed in this research. An EMEH ferromagnetic core material nonlinear characteristic will be taken into account in the design stage of the proposed work in order to provide a quick and accurate analytical model with various design parameters for production in a MATLAB environment. By examining the Norton equivalent circuit of the EMEH with a nonlinear Norton equivalent inductance, the nonlinear model may be obtained. With the nonlinear model design data, a prototype is built to evaluate the Norton equivalent circuit characteristics, AC-DC conversion, and the maximum power transfer from the EMEH using the discontinuously conducting DC-DC converters.

Rathore, B., etal (2021), In the power system, fault analysis (detection, classification, and localization) is critical. WAN (Wavelet, Alienation, and Neural) is a new method for analysing faults in UPFC compensated transmission networks. To identify and classify distinct outages, wavelet-based approximation coefficients calculated from current signals are employed. To pinpoint defects, an Artificial Neural Network is provided with approximated approximation

coefficients obtained from voltage and current data from the same quarter-cycle. There are many case studies in which the algorithm's resilience has been shown by modifying the parameters such as the position and frequency of the sampling, the system characteristics, noise effects, the angle of the fault initiation, and various control schemes and fault paths.

Kothari, N. H., etal (2020), Thyristor Controlled Series Compensator (TCSC)-based transmission lines are the focus of this article, which outlines a fault categorization and fault section identification strategy. Support Vector Machine (SVM) classifiers have been used to categorise faults and detect problematic sections based on instantaneous current data. Using PSCAD/EMTDC, a 400kV, 300km long, TCSC transmission line with sources at both ends was modelled in order to test the suggested technique. 3,840 failure examples were used to train the SVM classifier. A 99.83% accuracy rate was attained for fault classification and defective section identification using the suggested technique after testing 14,400 fault cases with a variety of malfunction and system scenarios.

Taheri, R., etal. (2020), Capacitor protection systems have an impact on the performance of SCCTL protection functions. There are a number of safety features, including a fault finder. The single line to ground (SLG) fault, the most prevalent fault type in transmission systems, is the focus of this work, which proposes a fault localization technique in the SCCTLs that is very precise. Using just one phasor measurement from the defective line, the suggested method determines the fault site, making it a low-cost and high-reliability one. Since the suggested approach does not need a communication link to obtain distant data, it may be readily implemented on numerical relays. The sample window is shifted in the proposed approach to find the original defect sites following signal processing. In the end, the precise position of the fault is determined by combining the original data on fault sites with a strategy for removing outlier data. MATLAB and DIgSILENT tools are used to model the suggested method and implement the processing procedure. The findings suggest that the proposed strategy is accurate and efficient.

Karunanayake, C., etal. (2019), Wind turbines with doubly fed induction generators (DFIG) and series compensated transmission systems may reduce sub-synchronous resonance (SSR) using a nonlinear sliding mode control (SMC). The rotor side converter is controlled using the suggested way to reduce SSR while maintaining the DFIG's decoupled torque and reactive power management capability. The suggested technique is validated by simulations using a comprehensive DFIG wind turbine model from the RTDS platform. The controller was shown to be effective in damping SSR when tested at varied compensation levels and wind speeds.

Paul, S., & Chang, J. (2019), An EMEH (electromagnetic energy harvester) for use in a deicing robot on power transmission lines is proposed in the current study as a design procedure. For the EMEH, both silicon (Si) and nickel (Ni) steels have been employed in order to take use of their respective properties. A 3D finite element method (FEM) based model of the EMEH has been compared to an analytical model in this research under the identical design specification. The magnetic equivalent circuit model of the EMEH is used to derive the equivalent circuit parameters. An impedance matching and maximum actual power extraction from the EMEH may be achieved using a power optimization circuit that includes a capacitor and a buck-boost converter, as well as the settings for this circuit. A co-simulation design platform is constructed utilising the 3D-FEM and MATLAB linked in a python-based environment to test the EMEH

and its power optimization circuit. Co-simulation platform is used to verify charging of 15 V rechargeable battery.

Biswal, S., etal. (2018), A real-time analysis of a time-frequency based approach is provided for a transmission line with a midpoint-connected static synchronous compensator in order to provide differential protection (STATCOM). The online Hilbert-Huang transformation is used to estimate the discrete Teager energy (DTE) using the first intrinsic mode function derived from the decomposition of current signals from both ends of the transmission system. Differential DTEs from both ends are utilised to determine whether phase of the line is defective. EMTDC/PSCAD is used to simulate a midpoint STATCOM adjusted transmission line model for analysis. For various STATCOM modes of operation, test scenarios such as high fault resistance, fault inception angle, reverse power flow, saturation of the current transformer, and change in source impedance are developed. A cross-country failure in a double-circuit transmission system is also checked using this approach. The suggested method's dependability, speed, and practicality have been shown by comparing it to traditional methods.

Sharma, N., etal. (2018), The Hilbert-huang transform is used to detect and identify problematic phases in a three-phase series capacitor-compensated transmission line linked to a wind energy source. Single-ended fault current data is used in the suggested method. On the proposed design, tests have been run for a wide variety of faults, each of which has its own distinct set of fault characteristics. These characteristics include the type of fault, the location of the fault, the fault resistance, the fault onset time, and the ground resistance. Additionally, the ground resistance has been tested. The findings of the testing indicate that the approach that was recommended is reliable and advantageous.

Gajare, S., etal. (2017) analytical and dynamic simulations and relay configurations need proper model parameters of many aspects to provide exact results. Due to weather and age, it is required to verify transmission line parameters at intervals. Methods to estimate the parameters of series-compensated lines utilising synchronised time-domain data acquired by intelligent electronic devices at both ends of the line are presented in this study that are free of the compensation model. Disruption generates waves that propagate down a line, which are used to calculate its propagation constant, which is used to determine its resistance and impedance. Finally, the line's inductance and capacitance are determined.

Asenkane, M. J., & Carpanen, R. P. (2017) The Static Synchronous Series Compensator's resonant properties are examined in this work. If the SSSC may produce electrical resonance in the line, it has the ability to trigger subsynchronous resonance (SSR) in surrounding turbine-generator plants, according to frequency-domain features of line impedance. As part of PSCAD's detailed investigations, the IEEE FBM model is updated. Since the SSSC produces capacitive reactance at both the rated system frequency and at subsynchronous frequencies, it has the ability to excite the SSR.

Zhang, Y., etal. (2016) The distributed parameter line model is used to develop a novel two-terminal fault-location technique for series-compensated double-circuit transmission lines. The series compensator has two subroutines, one for the left and one for the right side of the series compensator. Because the sequence voltages estimated from two sides are equivalent at the fault site, the voltage of a series-compensated device is deleted in each subroutine. Fault

locator functions are designed to take use of the property that the transition resistance is completely non-resistive at the area of the malfunction. This method does not need that the kind of fault be known, and there are no issues with finding the location of the fault and eliminating the pseudoroot. The excellent accuracy of the proposed fault-location approach is confirmed in MATLAB by using PSCAD to create multiple fault instances under various situations.

Junior, etal. (2016), An algorithm based on phase components and a heuristic technique is presented in this study for the fault identification of series-compensated transmission lines. For better algorithmic responsiveness, the authors provide a mathematical model of series compensation that includes all the necessary details to appropriately depict its behaviour. Using the Alternative Transients Program, the authors created a series-compensated double-circuit transmission line to test their method. Accuracy is clearly evident from the findings.

Behera, S., etal. (2015), Shunt linked FACTS devices, such as STATCOM and SVC, may improve the transmission line's power transfer capabilities by being installed in the middle of the line. Impedance measurement errors in transmission line shunt FACTS devices are examined as a first case study. The real-time simulations are carried out using PSCAD. Analytical studies are used to compare the outcomes of various fault situations, different system conditions, and different fault locations.

Çapar, A., & Arsoy, A. B. (2015), New fault-finding algorithms are proposed in this study for transmission lines that have been compensated. If the fault occurred before or after the compensator position on the line, that fact is taken into account while doing the fault location calculations. Determine if the fault is in front of a compensator by using an estimated MOV impedance. Many different kinds of faults, as well as fault locations and fault resistance, were tested on a 380 kV transmission line using a series capacitor and MOV. The findings reveal that the algorithm correctly predicts the location of the defect in every situation.

Vyas, B. etal. (2014), A society's progress may be measured by looking at how much electricity each person uses on a per-capita basis now. As a consequence, electricity consumption has increased by multiples. This pushes power engineers to develop and transmit the most practicable power along the transmission line, which results in the installation of compensating devices since temperature restrictions are reached. The process of compensation introduces new properties into the system. This calls for a reevaluation of the standard safety practises that are already in place. Additionally, in order to arrive at the most effective method, this article assesses the relative benefits and drawbacks of several strategies. Modern procedures are given more weight. To make it easier for novice researchers to assess alternative methodologies, the literature has been broken down into sections.

Piyasinghe, L., etal. (2014), SSRs in Type-3 wind farms with thyristor-controlled series capacitors are detected using impedance model-based frequency domain analysis (TCSC). A dynamic phasor-based TCSC impedance model and its use in Type-3 wind energy systems for SSR analysis are two major contributions to this research. This work develops impedance models for TCSCs with variable firing angles and variable impedances. Nyquist stability criteria is used to compare SSR stability in a Type-3 wind farm with TCSC or fixed capacitor compensation, using the obtained impedance models. It is shown that TCSCs may eliminate SSR in Type-3 wind generator interconnection systems via the use of analytical models. An

impedance model-based time-domain simulation in MATLAB/SimPowerSystems validates the analytical conclusions achieved by impedance modelling.

Samantaray, S. R. (2013), It is proposed in this study that an ensemble of decision trees be used to find the location of a fault zone in a transmission line utilising the flexible ac transmission systems (FACTS) and the thyristor-controlled series compensator and unified power-flow controller. An efficient method for locating fault zones is provided by the random forests model's stack of decision trees. After the TCSC/UPFC, half-cycle post-fault current and voltage samples from the fault inception are employed as an input vector against the desired outputs of "1" and "-1" respectively. Fault data from a broad range of operational parameters of the power system network, including noise, is used to assess the algorithm's reliability and reaction time (3/4th cycle from the moment of the fault's onset). Using the RF model, the findings of this technique show that FACTS-based transmission lines may be reliably identified.

Varma, R. K., & Moharana, A. (2013), Large wind farms are progressively being integrated into transmission networks to transport bulk electricity, and series compensation is being investigated. The transmission infrastructure and the wind farm are both modelled in great detail using a linear state space. An in-depth examination of the SSR's induction generator effect and torsional interaction is conducted. Multiple double-cage induction generator wind turbines, both commercially available and experimentally tested, are the subject of research. Wind turbine generators of the same size are exposed to varying wind speeds, while turbines of various sizes are also subjected to the same wind speed.

Kadia, J. V., & Jamnani, J. G. (2012), Series compensation has long been utilised to increase the power transfer capabilities of transmission lines, thanks to advances in power electronics and control engineering. A multitasking controller, the TCSC is able to enhance the overall characteristics of an electrical power network under both normal and malfunctioning conditions. Modeling and analysis of the performance of the TCSC controller for different occurrences, such as a failure on a long transmission line or sub synchronous resonance, is the focus of this research. The open and closed loop modes of TCSC are studied. Software programme PSCAD 4.2 was used to verify the findings by comparing them to various power system parameter values.

Maturu, S., & Shenoy, U. J. (2010), The performance of distance relays is detailed in this article when they are used to transmission systems that are equipped with shunt FACTS devices, such as the Static Synchronous Compensator (STATCOM). The purpose of the research that has been presented is to analyse the efficiency of the distance relays in the event that STATCOM is installed in the centre of the transmission lines in order to manage the voltage. There is a presentation here of a thorough model of STATCOM and its control technique. The evaluation of the distance relay takes into account a variety of loading circumstances as well as potential fault sites. The defects emerge as a result of a wide variety of pre-fault loading circumstances. The research is carried out on both 400KV and 132KV systems, and the findings are reported thereafter. Simulation studies are performed with the use of a piece of software known as PSCAD/EMTDC that is designed for transient simulation.

Zhang, W. H., Lee, S. J., & Choi, M. S. (2010), The use of distance relay is very vital in the process of ensuring the safety of transmission lines. Due to the compensating effect, the adoption of

flexible AC transmission systems (FACTS) devices, such as the static synchronous compensator (STATCOM), might have an influence on the performance of the distance relay. On the basis of this study, new guiding principles for the establishment of various protection zones have been offered. Matlab/Simulink is used to create a model of a conventional 500 kV transmission system that makes use of STATCOM. Research is being done to investigate the effect that STATCOM has on distance protection schemes for a variety of fault kinds, fault locations, and system configurations. The effectiveness of the distance relay is assessed on the basis of the results of the simulation. Through the use of STATCOM, the establishing concept may be validated for the transmission line.

5. DISCRETIZATION OF NON-UNIFORM TRANSMISSION LINE

Figure 2, shows the basic differential equations governing the voltage and current along a transmission line that's distributed parameters R, L, G and C which are varying along the line. The differential equations of non-uniform transmissions line are given in equations (1) and (2)

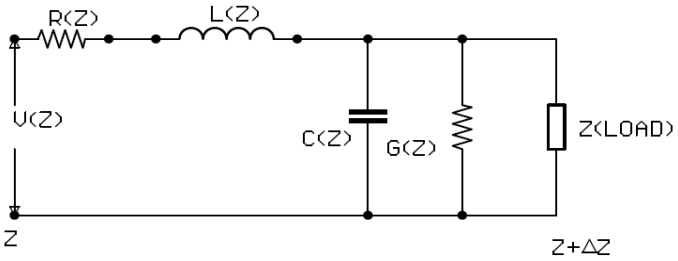

Figure 2: Discretization model of non-uniform transmission line

$$-\frac{dV(z)}{dz} = (R(z) + j\omega L(z)I(z) \quad (1)$$

$$-\frac{dI(z)}{dz} = (G(z) + j\omega C(z)V(z) \quad (2)$$

From equation (1)

$$I(Z) = -\frac{V'(z)}{R(Z)+J\omega L(Z)} \quad (3)$$

Substituting (3) into equation (2)

$$\frac{d}{dz}\left(\frac{V'(z)}{R(Z)+J\omega L(Z)}\right) = \big(G(Z) + J\omega C(Z)\big)V(Z) \quad (4)$$

$$\left(\frac{V'(z)}{R(Z)+J\omega L(Z)}\right) - \left(\frac{R'(Z)+j\omega L'(Z)}{(R(Z)+J\omega L(Z))}V'(z) - \big(G(z) + j\omega L(z)\big) = 0 \quad (5)$$

Now we will calculate v' (z)

Where

$$\lambda^{2=}((G(z) + J\omega C(z)(R(z) + J\omega L(z)) \quad (6)$$

Where

λ^2= Function of z

Let

$$A(z) = \left(\frac{R'(Z)+j\omega L'(Z)}{(R(Z)+J\omega L(Z))}\right.$$

$$B(z) = \lambda^2$$

Where, $R(z) = R_0+R_1\sin(\beta z)$ (7)

$$L(z) = L_0+L_1\sin\left(\beta z + \frac{\pi}{6}\right) \quad (8)$$

$$C(z) = C_0+C_1\sin\left(\beta z - \frac{\pi}{6}\right) \quad (9)$$

$$G(z) = G_0+G_1\sin(\beta z) \quad (10)$$

Where

$$\beta = \frac{2\pi}{\lambda}, R_1 = \frac{R_0}{2}, L_1 = \frac{L_0}{2}, G_1 = \frac{G_0}{2}, C_1 = \frac{C_0}{2}$$

$1 \leq n \leq 100$

$\boldsymbol{\lambda}$=1/10

Discretize Equation (11) with step size Δ

Where $z=n\Delta$ n=0,1, 2…….N-1

$N\Delta=d$

$$\Delta = \frac{1}{100}$$

After this Discretization, this second order differential becomes a second order difference equation.

Initially condition $V_o=1$

Final condition (load) $V_n=Z< load >.I(d)$

Thereafter we can calculate I_d and V_n values for values of $\boldsymbol{\lambda}$.

6. PERTURBATION THEORY OF NON-UNIFORM TRANSMISSION LINE

Perturbation theory is applied to the solution of inhomogeneous transmission line equations. These line equations are

$$-v_{,z} = L(z)i_{,t} + R(z)i$$

$$-i_{,z} = C(z)v_{,t} + G(z)v$$

Where R (z), L (z), C (z), G (z) is the distributed parameters of the line. We assume that these

distributed parameters have a strong constant parts and a constant weak varying part.

$$R(z) = R_o + \epsilon . R_1(z)$$

$$L(z) = L_o + \epsilon . L_1(z)$$

$$G(z) = G_o + \epsilon . G_1(z)$$

$$C(z) = C_o + \epsilon . C_1(z)$$

Assume constant frequency ω. Then the line current and voltage phasor I (z), V (z) satisfy.

$$-V' = (R + j\omega L)I$$

$$-I' = (G + j\omega C)V$$

Or in matrix notation

$$-\frac{d}{dz}\begin{pmatrix} V(z) \\ I(z) \end{pmatrix} = \begin{pmatrix} 0 & R(z) + j\omega L(z) \\ G(z) + j\omega C(z) & 0 \end{pmatrix}\begin{pmatrix} V(z) \\ I(z) \end{pmatrix}$$

We can write

$$A(z) = \begin{pmatrix} 0 & R(z) + j\omega L(z) \\ 0 & G(z) + j\omega C(z) \end{pmatrix}$$

$$= A_0 + \epsilon A_1(z)$$

Where,

$$A_o = \begin{pmatrix} 0 & R_o + j\omega L_o \\ G_o + j\omega C_o & 0 \end{pmatrix}$$

$$A_1(z) = \begin{pmatrix} 0 & R_1(z) + j\omega L_1(z) \\ G_1(z) + j\omega C_1(z) & 0 \end{pmatrix}$$

Is a slowly varying matrix. We expend the solution in power of ϵ, i.e.

$$\begin{pmatrix} V(z) \\ I(z) \end{pmatrix} = \sum_{n=0}^{\infty} \varepsilon^n \begin{pmatrix} V_n(z) \\ I_n(z) \end{pmatrix}$$

Substituting this in to the governing differential equations with the notation $X_n(z) = (V_n(z), I_n(z))^T$ and equating equal powers of ϵ gives

$$X_0'(z) = A_o X_0(z)$$

$$X_n'(z) = A_o X_n(z) + A_1(z) X_{n-1}(z), n = 0,1,2 \ldots \ldots$$

The solution is

$$X_o(z) = \exp(zA_o)\, X_o(z)$$

$$X_n(z) = \int_0^z \exp\left((z-u)\, A_0\right) A_1(u) X_{n-1}(u) du, n \geq 1$$

Iterating this scheme we get

$$X_n(z) = \left(\int_{0<u_n<u_{n-1}<..<u_1<z} \varphi(z-u_1)A_1(u)\varphi(u_1-u_2)A_2(u) \dots \dots \varphi(u_{n-1} - u_1)A_1(u_n)\varphi(u_n)du_n du_{n-1} \dots .. du_1 \right) X(0)$$

Where, $\varphi(z) = \exp(zA_0)$, suppose that we have solved the problem up-to $0(\varepsilon^n)$. This approximate solution can be written as

$$X(z) \approx \Psi_n(z)X(0)$$

Where

$$\Psi_N(z) = I + \sum_{n=1}^{N} \varepsilon^N \left(\int_{0<u_n<u_{n-1}<..<u_1<z} \varphi(z-u_1)A_1(u_1) \dots \varphi(u_{n-1} - u_1)A_1(u_n)\varphi(u_n)du_n du_{n-1} \dots .. du_1 \right)$$

The 2×2 matrices $\Psi_N(z)$for various values of zϵ[0,d] are computed by approximating the multiple integrals with discrete sums. For example,

$$\Psi_N(k) \approx I + \sum_{n=1}^{N} \varepsilon^N \Delta^n \left(\int_{0<k_n<k_{n-1}<..<k_1<k} \varphi(k-k_1)A_1(k_1) \dots \varphi(k_{n-1} - k_n)A_1(k_n)\varphi(k_n) \right)$$

Where $\Delta = (d|k)$ and. In other words, the entire length has been divided into K equal's part and the k=0,1 ,2,3……k-1 multiple integral has been replaced by a multiple sum.

Where, $Z = n\Delta$

$$N = 0,1,2 \dots \dots \dots \dots \dots \dots \dots N-1$$

$$N\Delta = d, \Delta = 1 \div 100$$

$$R_1(z) = \sin\left(\left(2 * \pi * \frac{n}{100}\right)\right)$$

$$L_1(z) = \sin\left(((2 * \pi * n)/(100 + \frac{x}{y})\right)$$

$$C_1(z) = \sin\left(((2 * \pi * n)/(100 - \frac{x}{y})\right)$$

7. SIMULATED RESULTS OF DISCRETIZATION METHOD

We have simulated the propagation of voltage along a transmission line having non-uniform distributed parameters. We started by writing down the basic transmission line equations by applying KVL and KCL to infinitesimal section of the line. Then eliminating the current variable, we arrived at a single second order linear ordinary differential equation with non-constant coefficient for the voltage phase at a given frequency. We approximated that differential equation by a difference equation and solved it using MATLAB. Our simulation results show the voltage along the line as a function of the distance from the source and frequency variable. Figure 3 shows the plot of voltage with distance (z) when the distributed parameters and frequency both are constant. This shows that the voltage is decreasing exponentially w.r.to distance (z). Figure 4 shows the plot of voltage with distance (z) when the distributed parameters are non-constant but frequency is constant. This shows that the decrease in voltage variation w.r. to distance (z) is exponential. Figure 3 shows the three dimensional plot of the voltage phasor as a function of both the variables frequency and distance from the source end. This shows that there is variation in voltage in normalized distance range of 0 to 50 but in the normalized frequency range of 0 to100 there is no more variation in voltage. This three dimensional plot can be used to determine spectral density of voltage waveform along the line when the input voltage is a stationary random-process. This can be used to estimate the distributed parameters from measurement of correlation of the voltage waveform along the line. We have considered six different cases for both fixed values and varying values of primary constants. The corresponding simulated results are given in Figures 5-10.

The cases are given below

Case 1: When $1/RC = 1/\sqrt{LC}$ where variations are in the primary constants derived from Equations (11)-(14) with normalized frequency and distance both. Result for the case is already discussed by using the Figure below.

Case 2: When $1/RC >> 1/\sqrt{LC}$ where variations are in the primary constants derived from Equations (12)-(15) with normalized frequency and distance both. Figure 7 illustrates three dimensional plot of the voltage phasor as a function of both the variables frequency and distance from the source end. This shows that there is voltage strength in normalized distance range from 0 to 35 and negligible in remaining distance range but in the normalized frequency range of 55 to 75 voltage strength is decreasing, at starting and at the end, it is increasing.

Case 3: When $1/RC << 1/\sqrt{LC}$ where variations are in the primary constants derived from Equations (12)-(15) with normalized frequency and distance both. From Figure 8 it is observed that the results are almost similar as in case 1 or Figure 6.

Case 4: When $1/RC = 1/\sqrt{LC}$ for fixed primary constants with normalized frequency and distance both. Figure 9 illustrates a three dimensional plot of the voltage phasor as a function of the variables, frequency and distance from the source end. This shows that the voltage strength is compared to other cases mentioned above is high for all normalized distances.

Case 5: When $1/RC >> 1/\sqrt{LC}$ for fixed primary constants with normalized frequency and distances both. Figure 10 illustrates three dimensional plot of the voltage phasor as a function of both the variables frequency and distance from the source end. This shows that there is variation in voltage in normalized distance range of 0 to 70 and above the distance range 70

voltage strength is negligible but in the normalized frequency range of 0 to10 variations in voltage is negligible and after that there is a comparatively high strength.

Case 6: When 1/RC << 1/√LC for fixed primary constants with normalized frequency and distances both. From Figure 10 it is observed that the results are almost similar as in case 4 or Figure 8.

Case7: When 1/RC >> 1/√LC for fixed practical values of primary constants with normalized frequency and distances both.

Case8: When 1/RC << 1/√LC where variations in practical values are in primary constants derived from equation (13-16) with normalized frequency and distances both.

Case9: Voltage variations with distance (z) when $\omega = 1, \omega = 3, \omega = 6, \omega = 10, \omega = 12$.

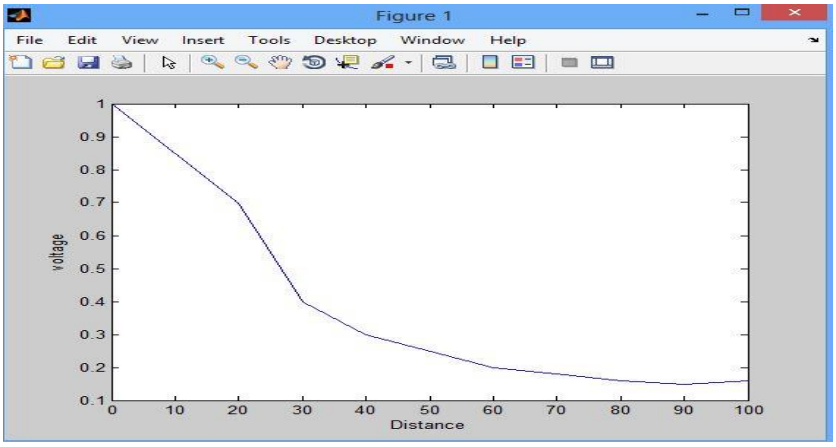

Figure 3: Voltage variation with normalized distance (z) for fixed frequency but varying primary constants.

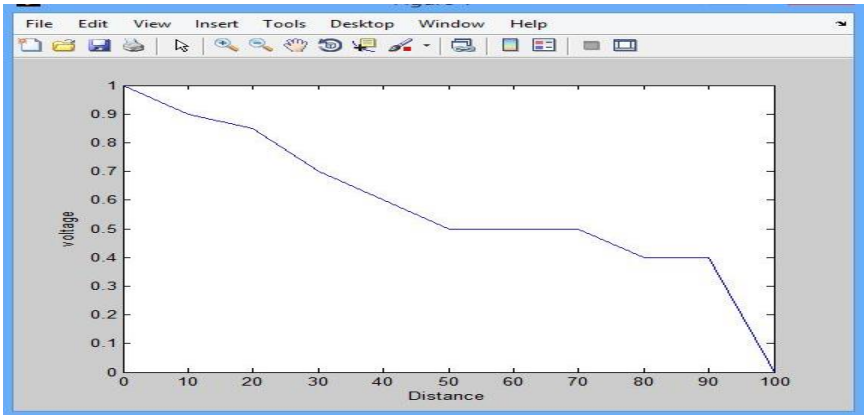

Figure 4: Voltage variation with normalized distance (z) for fixed frequency and primary constants

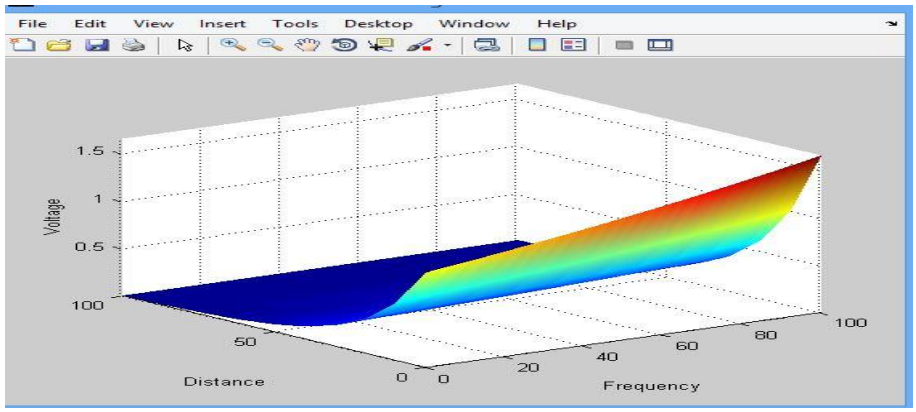

Figure 5: Voltage variations with normalized frequency and distance for the variable primary constants ($1/RC \gg 1/LC$)

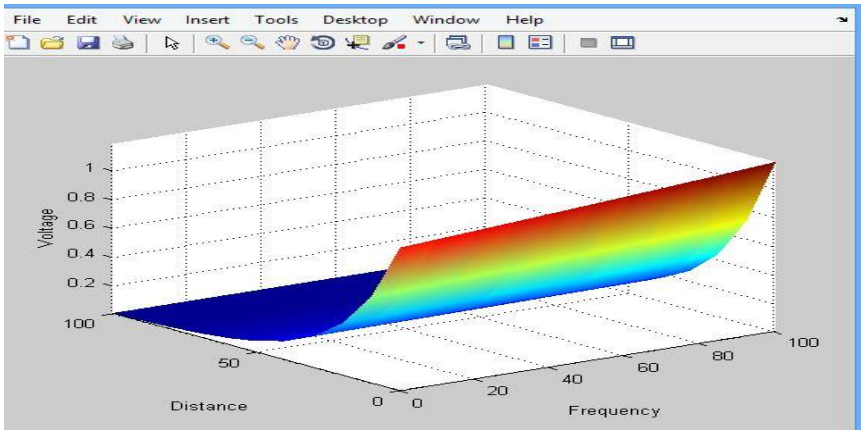

Figure 6: Voltage variations with normalized frequency and distance for the variable primary constants ($1/R=1/LC$)

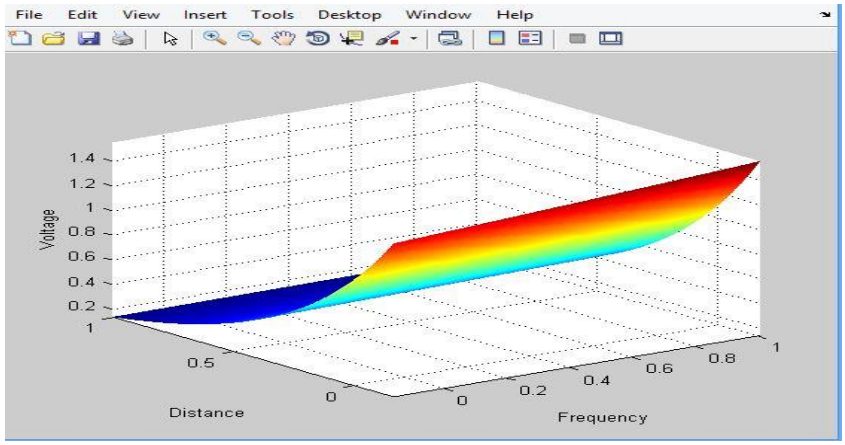

Figure 7: Voltage variations with normalized frequency and distance for the variable primary

constants (1/RC ≪ 1/LC)

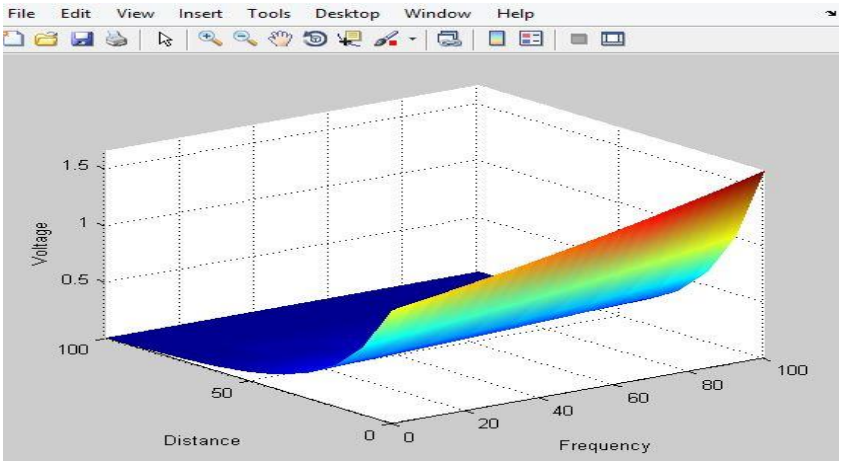

Figure 8: Voltage variations with normalized frequency and distance for the fixed primary constants (1/R=1/LC)

8. SIMULATED RESULT OF PERTURBATION METHOD

In our method we consider the non-uniform transmission line and we have simulated the propagation of voltage along this line which have distributed a small perturbated parameter ϵ is attached to this weak varying part. We expand the voltage and current in power of ϵ and solved in form of differential equation by Dyson series which is analogous to that used in perturbated theoretical quantam mechanics. Simulations are carried out using MATLAB. The result shows that the voltage along the line is a function of distance from the source and frequency variable. Figure 7 present the plot between the voltage and distance. (i.e. voltage w.r.to distance), where the constant part having the values are R_0=1, L_0=1, C_0=1, G_0=1 but there is no change in the varying part of the primary constant at a fixed normalized frequency ω=1. This shows that first voltage rise than decrease and rise w.r. to different normalized values of the distance (z). The maximum peak voltage is at 50, the value of normalized distance (z) than after it decreases for the range of normalized distance 90 to 100. There another change in voltage means that the voltage will rise after the normalized distance (z) value of 95. Figure 4 shows the three dimensional plot of voltage phasor as a function of both the variable frequency and distance from the source end. The constant part of the primary constant contains the values of R_0=1, L_0=1, C_0=1, G_0=1 but there is no change in the varying part of the primary constants.

This figure present that there exist the voltage strength in the whole normalized distance range but for the frequency range of 0 to 20 the voltage strength is decreasing at the starting but there after there is a good voltage strength. Figure 5 show that the three dimensional plot f voltage phasor as a function of both the variable frequency and the distance from the source end. Constant part contain the value ofR_0=1, L_0=100, C_0=1, G_0=1 but the varying part will remain same. From the figure we can conclude that there exist voltage strength for the whole range of the normalized distance but for the normalized frequency range of 0 to 10 voltage strength is

decreasing at the starting but after that there is good voltage strength.

Figure 6 shows three dimensional plot of the voltage phasor as a function of both the variables frequency and distance from the source end. The constant art contains the values of R_0=1, L_0=0.01, C_0=1, G_0=1and the varying part remain same. This figure shows that there exists voltage strength for the whole range of normalized distance but at the starting normalized frequency voltage strength is weak and after this there is good voltage strength. Figure 7 shows the two dimensional plot of the voltage phasor as a function of distance from the source end for different fixed frequencies for ω= 10, 25, 1, 50, 75, 100. Constant part contains the values ofR_0=1, L_0=1, C_0=1, G_0=1 and the varying part will remain same. This figure shows that with increase in the normalized frequency the voltage strength will also increase. Better voltage can be seen that when the frequency ω=25, 50, 75, 100. Or we can say that the voltage strength is weak for the lower range of normalized frequency. This type of transmission lines can be used for high frequencies systems.

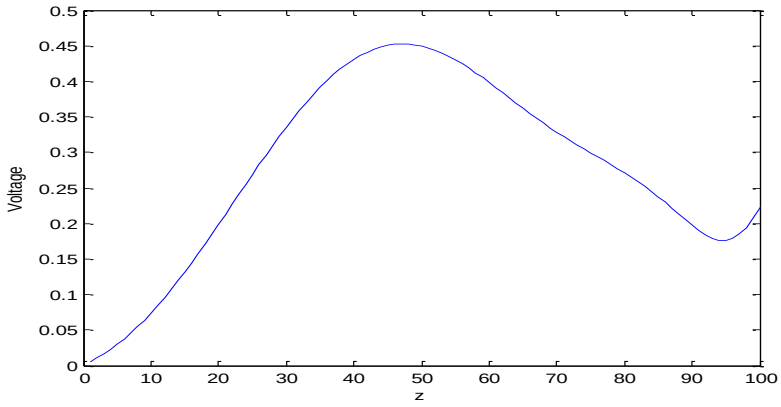

Figure 9: Voltage variation with normalized frequency (ω=1) but values of constant part ofR_0= 1, L_0= 1, C_0=1, G_0=1 and varying part is same

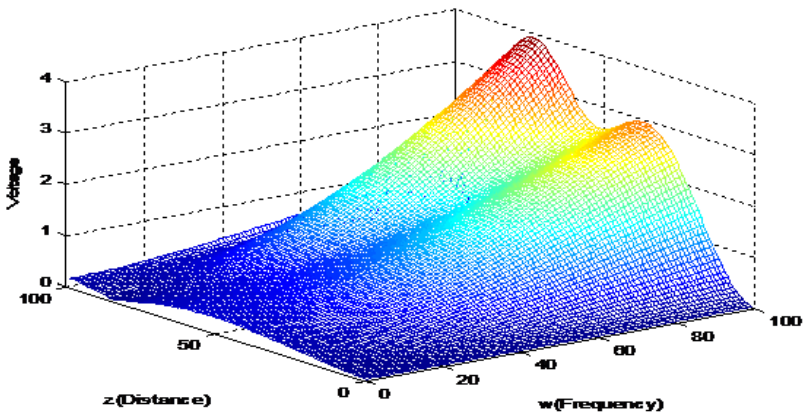

Figure 10: Voltage variation with normalized distance (z) for fixed frequency (ω=1) but

values of constant part of primary constants are R_0= 1, L_0= 1, C_0=1, G_0=1 and varying part is same

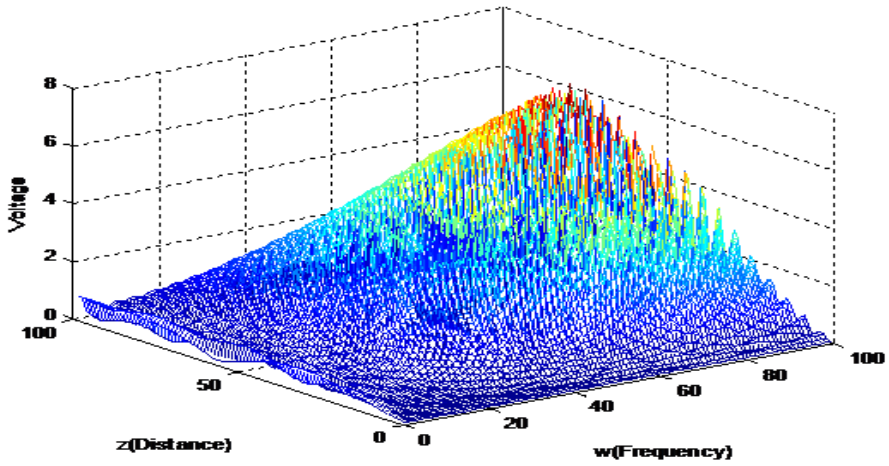

Figure 11: Voltage variation with normalized Distance (z) for fixed frequency (ω) but values of constant parts of primary constants are R_0= 1, L_0= 100, C_0=1, G_0=1 and varying part is same

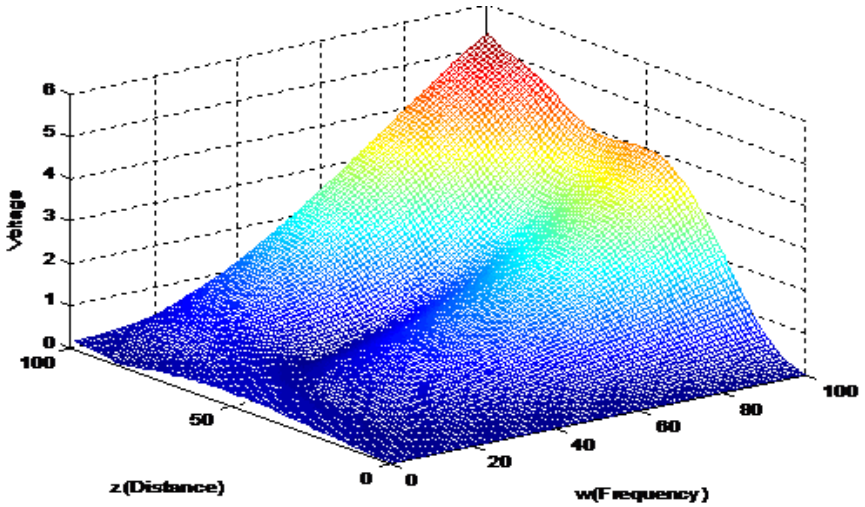

Figure 12: Voltage variation with normalized distance (z) for fixed frequency (ω) but values of constant part of constants are R_0= 1, L_0= 0.01, C_0=1, G_0=1 and varying part is same

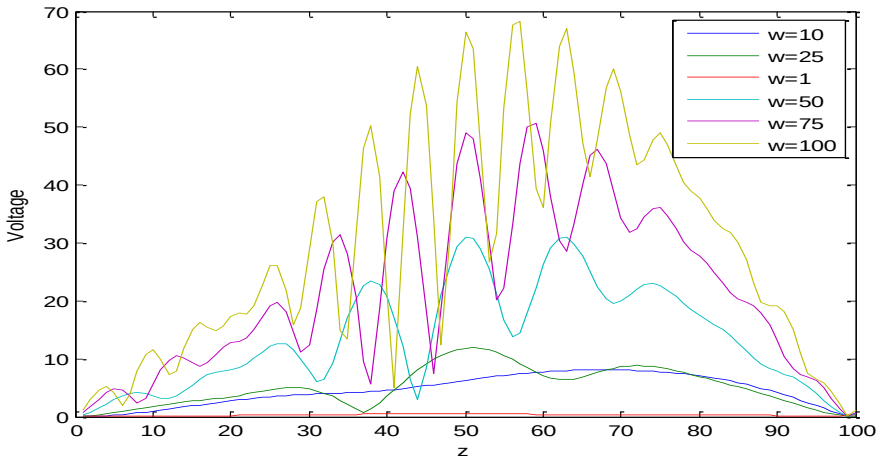

Figure 13: Voltage variation with normalized distance (z) for fixed frequency ω=10, 25, 1, 50, 75, 100 but values of constant part of primary constants are R_0= 1, L_0= 0.01, C_0=1, G_0=1 and varying part is same

9. CONCLUSION

This type of transmission line can be used for high frequencies systems. In summary, the successful approximation using the perturbation method is achieved provided the amplitudes of the distributed parameters are not too large. The most far reaching generalization of the work is carried out in this thesis is the following. The distributed parameters along the line are nonlinear function of voltage and current histories up to time t. Models for these dependencies can be obtained by

(a) By considering the B-H hysteresis curve which gives the inductance as a functional of the past current values.

(b) By considering ohmic heating of the resistances cause the temperature changes in the resistances there by affecting the resistance values. Since ohmic temperature increment depends on the past $i^2(t)$ values it follows that the resistance are also functional or the past current values. The transmission line equations then become a set of non linear integral differential equations and perturbation methods are need to be developed to solve these equations.

(c) Non uniform Transmission lines with randomly fluctuating parameters.

In Modeling file it is been created a short transmission line which has parameter as discussed above. It has clearly shows that the output graph of frequency becomes linear just after the simulation starts. It has clear that the transmission line has stable output and very less distortion.

References

1. Jagadeesh Kumar, M., Muthamizhan, T., Rathnavel, P., Ezhilarasan, G., & Eswaran, T. (2022). Performance and Analysis of Voltage Compensation in Transmission Line Using SMES-Based IDVR. In Proceedings of International Conference on Power Electronics and Renewable Energy Systems (pp. 613-623). Springer, Singapore.
2. Saad, M., & Kim, C. H. (2022). Unscented-Kalman-filter-based single-phase adaptive reclosing of shunt-compensated extra-high-voltage transmission lines. Alexandria Engineering Journal.
3. Paul, S., Lee, D., Kim, K., & Chang, J. (2021). Nonlinear modeling and performance testing of high-power electromagnetic energy harvesting system for self-powering transmission line vibration deicing robot. Mechanical Systems and Signal Processing, 151, 107369.
4. Rathore, B., Mahela, O. P., Khan, B., & Padmanaban, S. (2021). Protection scheme using wavelet-alienation-neural technique for upfc compensated transmission line. IEEE Access, 9, 13737-13753.
5. Kothari, N. H., Bhalja, B. R., Pandya, V., & Tripathi, P. (2021). A rate-of-change-of-current based fault classification technique for thyristor-controlled series-compensated transmission lines. International Journal of Emerging Electric Power Systems.
6. Taheri, R., Eslami, M., & Damchi, Y. (2020). Single-end current-based algorithm for fault location in series capacitor compensated transmission lines. International Journal of Electrical Power & Energy Systems, 123, 106254.
7. Karunanayake, C., Ravishankar, J., & Dong, Z. Y. (2019). Nonlinear SSR damping controller for DFIG based wind generators interfaced to series compensated transmission systems. IEEE Transactions on Power Systems, 35(2), 1156-1165
8. Paul, S., & Chang, J. (2019). Design of novel electromagnetic energy harvester to power a deicing robot and monitoring sensors for transmission lines. Energy conversion and management, 197, 111868.
9. Biswal, S., Biswal, M., & Malik, O. P. (2018). Hilbert Huang transform based online differential relay algorithm for a shunt-compensated transmission line. IEEE Transactions on Power Delivery, 33(6), 2803-2811.
10. Sharma, N., Ali, S., & Kapoor, G. (2018, September). Fault detection in wind farm integrated series capacitor compensated transmission line using Hilbert Huang transform. In 2018 International Conference on Computing, Power and Communication Technologies (GUCON) (pp. 765-769). IEEE.
11. Gajare, S., Pradhan, A. K., & Terzija, V. (2017). A method for accurate parameter estimation of series compensated transmission lines using synchronized data. IEEE Transactions on Power Systems, 32(6), 4843-4850.
12. Zhang, Y., Liang, J., Yun, Z., & Dong, X. (2016). A new fault-location algorithm for series-compensated double-circuit transmission lines based on the distributed parameter model. IEEE Transactions on Power Delivery, 32(6), 2398-2407.
13. Junior, G. M., Di Santo, S. G., & Rojas, D. G. (2016). Fault location in series-compensated transmission lines based on heuristic method. Electric Power Systems Research, 140, 950-957.
14. Behera, S., Raja, P., & Moorthi, S. (2015, December). Modelling and simulation of the impact of SVC on existing distance relay for transmission line protection. In 2015 International Conference on Condition Assessment Techniques in Electrical Systems (CATCON) (pp. 151-156). IEEE.
15. Çapar, A., & Arsoy, A. B. (2015). A performance oriented impedance based fault location algorithm for series compensated transmission lines. International Journal of Electrical Power & Energy Systems, 71, 209-214.
16. Vyas, B., Maheshwari, R. P., & Das, B. (2014). Investigation for improved artificial intelligence techniques for thyristor-controlled series-compensated transmission line fault classification with discrete wavelet packet entropy measures. Electric Power Components and Systems, 42(6), 554-

566.
17. Piyasinghe, L., Miao, Z., Khazaei, J., & Fan, L. (2014). Impedance model-based SSR analysis for TCSC compensated type-3 wind energy delivery systems. IEEE Transactions on Sustainable Energy, 6(1), 179-187.
18. Samantaray, S. R. (2013). A data-mining model for protection of FACTS-based transmission line. IEEE Transactions on Power Delivery, 28(2), 612-618.
19. Varma, R. K., & Moharana, A. (2013). SSR in double-cage induction generator-based wind farm connected to series-compensated transmission line. IEEE transactions on power systems, 28(3), 2573-2583.
20. Song, G., Chu, X., Gao, S., Kang, X., Jiao, Z., & Suonan, J. (2013). Novel distance protection based on distributed parameter model for long-distance transmission lines. IEEE transactions on power delivery, 28(4), 2116-2123.
21. Suonan, J., Zhang, J., Jiao, Z., Yang, L., & Song, G. (2013). Distance protection for HVDC transmission lines considering frequency-dependent parameters. IEEE Transactions on Power Delivery, 28(2), 723-732.
22. Eristi, H. (2013). Fault diagnosis system for series compensated transmission line based on wavelet transform and adaptive neuro-fuzzy inference system. Measurement, 46(1), 393-401.
23. Moharana, A., Varma, R. K., & Seethapathy, R. (2012, July). SSR mitigation in wind farm connected to series compensated transmission line using STATCOM. In 2012 IEEE Power Electronics and Machines in Wind Applications (pp. 1-8). IEEE.
24. Rahmani, M., Vinasco, G., Rider, M. J., Romero, R., & Pardalos, P. M. (2013). Multistage transmission expansion planning considering fixed series compensation allocation. IEEE Transactions on Power Systems, 28(4), 3795-3805.
25. Abdelaziz, A. Y., Mekhamer, S. F., & Ezzat, M. (2013). Fault location of uncompensated/series-compensated lines using two-end synchronized measurements. Electric power components and systems, 41(7), 693-715.
26. Suriyaarachchi, D. H. R., Annakkage, U. D., Karawita, C., Kell, D., Mendis, R., & Chopra, R. (2012, July). Application of an SVC to damp sub-synchronous interaction between wind farms and series compensated transmission lines. In 2012 IEEE Power and Energy Society General Meeting (pp. 1-6). IEEE.
27. Kadia, J. V., & Jamnani, J. G. (2012). Modelling and analysis of TCSC controller for enhancement of transmission network. International Journal of Emerging Technology and Advanced Engineering, 2(3), 223.
28. Maturu, S., & Shenoy, U. J. (2010, October). Performance issues of distance relays for shunt FACTS compensated transmission lines. In 2010 International Conference on Power System Technology (pp. 1-6). IEEE.
29. Zhang, W. H., Lee, S. J., & Choi, M. S. (2010). Setting considerations of distance relay for transmission line with STATCOM. Journal of Electrical Engineering and Technology, 5(4), 522-529.
30. Shah, A., Sood, V. K., & Saad, O. (2009, June). Mho relay for protection of series compensated transmission lines. In International Power System Transients Conference.
31. Dambhare, S., Soman, S. A., & Chandorkar, M. C. (2009). Adaptive current differential protection schemes for transmission-line protection. IEEE Transactions on Power Delivery, 24(4), 1832-1841.